International Journal of Nanoelectronics and Materials
Volume 13 (Special Issue) Dec 2020 (225-234)

First-Principles Study on the Doping Effects of La on the Structural, Electronic and Optical Properties of MgO

M. F. M. Taib[1,6*], M. H. Samat[6], S. Z. N. Demon[2], N. H. Hussin[3], O. H. Hassan[4, 6], M. Z. A. Yahya[5, 6] and A. M. M. Ali[1, 6]

[1]*Faculty of Applied Sciences, Universiti Teknologi MARA (UiTM), 40450 Shah Alam, Selangor, Malaysia.*
[2]*Centre for Defence Foundation Studies, National Defence University of Malaysia, 57000 Kuala Lumpur, Malaysia.*
[3]*Faculty of Applied Sciences, Universiti Teknologi MARA (UiTM), 26400 Jengka, Pahang, Malaysia.*
[4]*Department of Industrial Ceramics, Faculty of Art & Design, Universiti Teknologi MARA (UiTM), 40450 Shah Alam, Selangor, Malaysia.*
[5]*Faculty of Defence Science & Technology, Universiti Pertahanan Nasional Malaysia, 57000 Kuala Lumpur, Malaysia.*
[6]*Ionic Materials & Devices (iMADE) Research Laboratory, Institute of Science, Universiti Teknologi MARA (UiTM), 40450 Shah Alam, Selangor, Malaysia.*

ABSTRACT

The structural, electronic and optical properties of pure MgO and La-doped MgO were investigated by first-principles study based on density functional theory (DFT). The good agreement of the calculated lattice parameters of MgO with experimental and other theoretical data was obtained. It was found that the calculated band gap of MgO using LDA functional is 4.756 eV and the presence of La impurity in MgO decreases the band gap to 1.812 eV. The high contribution of La 5d state was found at conduction band while the main peak of valence band is represented by O 2p state. The optical properties for the absorption coefficient with and without scissor operator (SO) were also presented and compared with the optical absorption spectra from experimental data. The red-shift of the absorption was obtained which show that the La doping can extend the absorption range in MgO. These findings would be useful for understanding the behavior of MgO and La-doped MgO for promising material in photocatalyst application.

Keywords: First-Principles, Density Functional Theory, MgO, La Doping, Impurity.

1. INTRODUCTION

Magnesium oxide (MgO) as nanostructures material is a technologically important material. In the last few years, there is an extensive study on MgO due to its non-toxicity, low cost, high-temperature resistance, high optical transmittance and one of the most abundant minerals on Earth [1]. Nowadays, some applications such as chemical sensors and solar cells using MgO [2, 3]. MgO also plays a role in electronic and optoelectronic devices for the laser and light-emitting diodes (LEDs) especially for blue or green light emitters [4, 5]. Many superconductor products also using MgO as a catalyst and substrate [6]. Normally, perfect MgO crystallizes in the cubic rocksalt structure where the cations are surrounded by octahedral anions with filled valence *p* bands. The Mg is in a 2+ state as its two electrons are transferred to the neighbor O atom, which is in a 2– state [7]. The band gap of MgO is very large at 7.8 eV that falls into deep ultraviolet (UV) region [8]. Therefore, there is a need to adjust the optical absorption spectra of MgO especially for solar cell and photocatalyst applications.

*Corresponding Author: *mfariz@uitm.edu.my*

To date, several studies have been conducted to investigate the properties of pure MgO [9–11] and doped-MgO [12–15]. Recently, Vaizoğullar [16] reported the La-doped MgO for photocatalyst. The obtained results conclude that La^{+3} can remarkably increase the photocatalytic performance of MgO.

Previous first-principles studies have reported the use of La dopant in metal oxide such as ZnO [17–20], SnO_2 [21], TiO_2 [22, 23] and other materials [24–28]. The previous reported on the La-doped ZnO by Deng et al. [18] and Peng et al. [19] showed that the wider energy gap was achieved in the ZnO system with La doping. Thus, the blue shift of absorption threshold was obtained. Changpeng Chen and Meilan Qi [21] studied La-doped SnO_2 and the results revealed the red-shifts in the absorption spectra due to the effective reduction of the band gap of SnO_2 after doping with La. For La-doped TiO_2, the band gap decreased with the increase of the La doping level as reported by Huang *et al.* [22]. The band gap narrowing will cause an enhancement of visible-light absorption and photocatalytic performance. However, to the best of our knowledge, the first-principles study on the properties of La-doped MgO has not been reported.

In this work, the structural properties (lattice parameters, volume, bond length and formation energy) electronic properties (band structure and density of states) and optical properties (absorption coefficient) of pure MgO in cubic structure and the effect of La doping on the properties of MgO were reported and discussed. The first-principles calculations were performed to understand the properties of MgO and the role of La impurity in MgO.

2. COMPUTATIONAL METHOD

The calculations on structural, electronic and optical properties of MgO and La-doped MgO were performed using density functional theory (DFT) based on plane wave ultrasoft pseudopotential approach. All of the calculations were implemented using the Cambridge Serial Total Energy Package (CASTEP) computer code [29]. The local density approximation by Ceperley and Adler [30] as parametrized by Perdew and Zunger [31] (LDA-CAPZ) and generalized gradient approximation by Perdew-Burke-Ernzerhof (GGA-PBE) [32] and Perdew-Burke-Ernzerhof for solids (GGA-PBEsol) [33] were used for the exchange-correlation. The wave function was expanded as much as 400 eV plane wave cutoff energy and *k*-points of 4×4×4 to ensure to ensure good convergence results. The valence electron configurations were treated as $2p^6\ 3s^2$ for Mg, $2s^2\ 2p^4$ for O and $5p^6\ 5d^1\ 6s^2$ for La. The geometrical optimization was performed using the total energy of 5.0×10^{-6} eV/atom, maximum force of 0.01 eV/Å, maximum stress of 0.02 GPa and maximum atomic displacement of 5.0×10^{-4} Å.

3. RESULTS AND DISCUSSION

3.1.1 Structural Properties

MgO has the rocksalt crystal structure with cubic structure (space group: Fm3m, No. 225) as visualized in Figure 1. The structural properties of MgO were studied in terms of lattice parameters, cell volumes and also the bond lengths. The lattice parameters and volumes of the optimized structure of pure MgO were calculated using LDA, GGA-PBE and GGA-PBEsol as listed in Table 1 to validate the best functional of the calculations. The reliability of the computational method was approved by comparing the structural properties of MgO with experimental data. The results indicate that the LDA functional provides the best agreement with the experimental data by 0.14% for lattice parameters and 0.41% for volume compare to GGA-PBE and GGA-PBEsol. The present results were also consistent with other theoretical calculations from various methods and software.

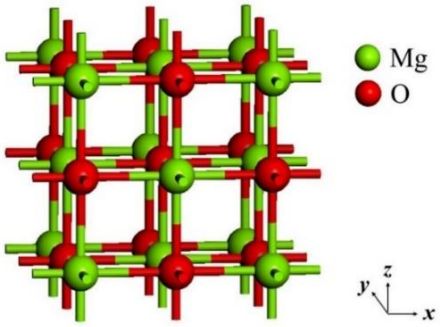

Figure 1. Crystal structure of pure MgO.

Table 1 Lattice parameter (a = b = c) and volume (V) of pure MgO (Fm3m, No. 225) from theoretical and experimental data

Method	a (Å)	V (Å^3)	Software
LDA	4.206 (-0.14%)	74.41 (-0.41%)	CASTEP
GGA-PBE	4.298 (+2.04%)	79.37 (+6.22%)	CASTEP
GGA-PBEsol	4.268 (+1.33%)	77.77 (+4.08%)	CASTEP
LDA [34]	4.240	76.20	ABINIT
GGA-PBE [35]	4.270	77.85	CASTEP
GGA-PBE [36]	4.237	76.06	VASP
GGA-PBEsol [37]	4.22	75.15	WIEN2k
Experiment [38]	4.212	74.72	-

The La-doped MgO was constructed by replacing one of the Mg atoms with La atom as illustrated in Figure 2. The unit cell of MgO consists of 4 Mg atom and 4 O atom. There are 4 different positions of Mg that can be replaced by La. Therefore, the most stable position of La was searched by calculating the formation energy of La doping in MgO at different doping positions as shown in Figure 3. According to the law of energy conversion, the difference between the energy of the systems after and before the replacement is called formation energy. In this work, the formula of formation energy is referred to the formalism defined by Chen et al. [39]. The formation energy, E_f of La-doped MgO was calculated by:

$$E_f = E_{\text{La: MgO}} + E_{\text{Mg}} - \left(E_{\text{MgO}} + E_{\text{La}}\right) \quad (1)$$

where $E_{\text{La: MgO}}$ is the total energy of La-doped MgO, E_{MgO} is the total energy of pure MgO and E_{Mg} and E_{La} represent the energy of single Mg atom and La atom, respectively. The favorable position for La doping in MgO according to its formation energy is at P4 due to its lowest formation energy. The position at P4 is more stable than other positions with E_f = 7.842778620 eV. Therefore, the calculations for the structural, electronic and optical properties of La-doped MgO have been performed with these structure.

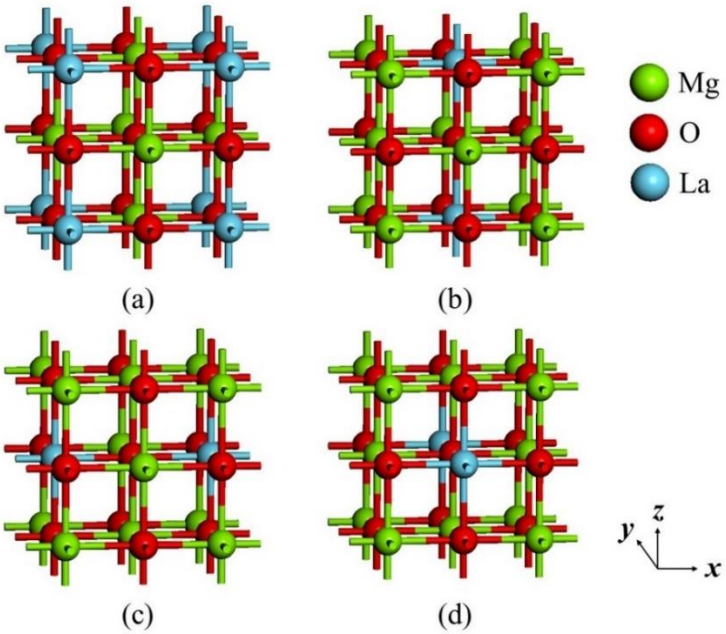

Figure 2. Crystal structures of La-doped MgO with different doping position (a) P1, (b) P2, (c) P3 and (d) P4.

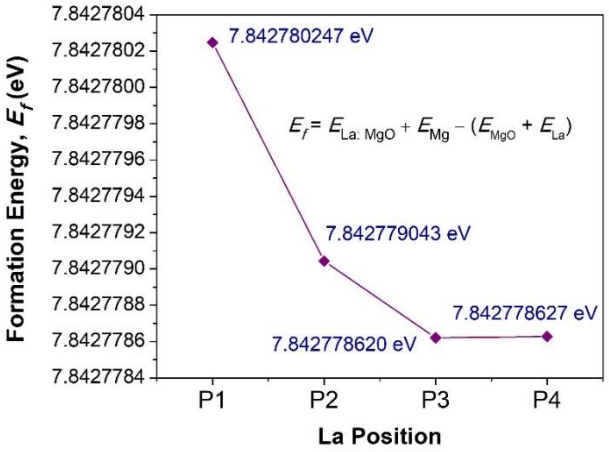

Figure 3. Formation energy of La-doped MgO in different La positions.

The lattice parameters, volume and bond length of pure MgO and La-doped MgO from LDA functional are listed in Table 2. After La doping in MgO, the lattice parameters and volumes induces a more significant lattice expansion with a unit cell volume of 106.16 Å^3 which increased by 42.67%. The bond length of Mg-O in La-doped MgO is longer than pure MgO while La-O bond also has the same bond length with Mg-O as displayed in Figure 4. This is consistent with the fact that the ionic radius of the La atom (1.95 Å) that is larger than the Mg atom (1.45 Å).

Table 2 The lattice parameters, volume and bond length of pure MgO and La-doped MgO from LDA functional

Structures	*a* (Å)	V (Å^3)	Mg-O (Å)	La-O (Å)
Pure MgO	4.206	74.41	2.103	-
La-doped MgO	4.735	106.16	2.367	2.367

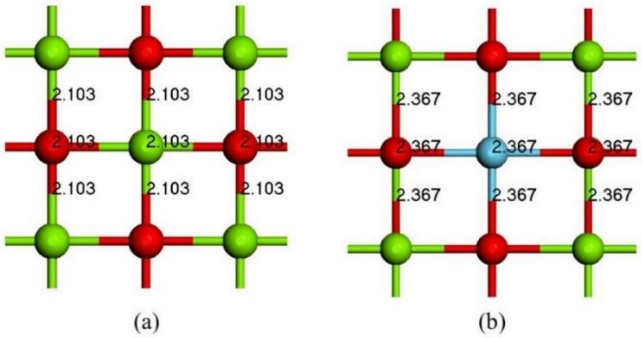

Figure 4. Bond length of Mg-O and La-O for pure MgO and La-doped MgO.

3.1.2 Electronic Properties

The calculated band gap of pure MgO using LDA, GGA-PBE and GGA-PBEsol with comparison to other theoretical and experimental band gaps as well as the band gap of La-doped MgO are listed in Table 3. It was found that the calculated band gap with LDA functional is higher than the calculations with GGA-PBE and GGA-PBEsol. The calculated direct band gap of pure MgO is consistent with other theoretical band gap using standard DFT in the range of 4.45 to 4.74 eV. It is well-known that the DFT method usually provides a significantly underestimated band gap value as compared to one that was obtained experimentally. This is because, the DFT only relates to ground-state properties and the band gap itself refers to an excited-state property, which standard DFT is unable to describe correctly. The local functional from LDA and GGA can result in poor for electronic band gap due to the lack of self-interaction corrections [40]. In this work, the calculated band gap is lower than the experimental band gap of 7.8 eV by 39% [41]. Thus, MgO requires a description beyond DFT such as a hybrid functional or DFT+U method [42], [43]. Although the band gap of MgO is lower than the experimental value, the discussion of this work remains unaffected since this is mainly focused on the relative improvement in MgO properties after doping with La.

The calculated electronic band structure of pure MgO and La-doped MgO along some high-symmetry lines in the Brillouin zone is shown in Figure 5. The Fermi level (indicated by a horizontal line) lies at zero energy. The calculated band gap of pure MgO at G point using LDA is 4.756 eV which is a direct band gap. It can be seen that the band gap of MgO after doping with La is reduced to 1.812 eV. The narrowing of the band gap of La-doped MgO is due to the presence of La state that causes the shift of the conduction band toward the lower energy region.

Table 3 The band gap of pure MgO and La-doped MgO

Structures	**Method**	E_g **(eV)**	**Software**
Pure MgO	LDA	4.756	CASTEP
	GGA-PBE	4.234	CASTEP
	GGA-PBEsol	4.276	CASTEP
	GGA-PBE [7]	4.74	WIEN2k
	GGA-PBE [44]	4.45	WIEN2k
	GGA-PW91 [42]	4.56	VASP
	Experiment [41]	7.8	-
	Experiment [8]	7.77	-
La-doped MgO	LDA	1.812	CASTEP

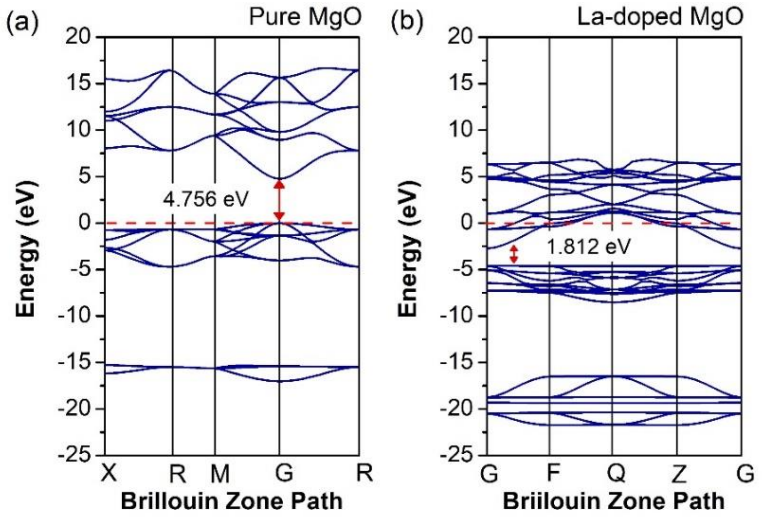

Figure 5. Band structures of (a) pure MgO and (b) La-doped MgO.

The partial and total density of states (DOS) was used to analyze the distribution of elements in each orbital and to identify the main peaks in the DOS whether they are from *s*, *p* or *d* character. The total and partial DOS of pure MgO and La-doped MgO are shown in Figure 6 while Figure 7 shows the total and partial DOS of all the atoms in MgO and La-doped MgO to provide further insight of DOS. For pure MgO, the valence band maximum is mainly contributed by O 2*p* state near the Fermi level while there is a small appearance of Mg 3*s* and Mg 2*p* states founds at the conduction band. For La-doped MgO, the Fermi level moved towards the conduction band due to the high contribution of impurity energy level (IEL) from La 5*d* state. This formation of the impurity energy of La leads to the band gap narrowing. A low contribution of La 5*d* state appears at the valence band while the high contribution of La 5*d* state can be seen at the bottom of the conduction band. This location of IEL made the IEL becomes a shallow donor level. This kind of IEL could act as a trap center for photoexcited holes or electrons which could reduce the recombination rate. The La 5*d* states at the conduction band overlap with O 2*p* states, indicating a strong exchange interaction between them. This strong interaction causes the splitting of energy levels.

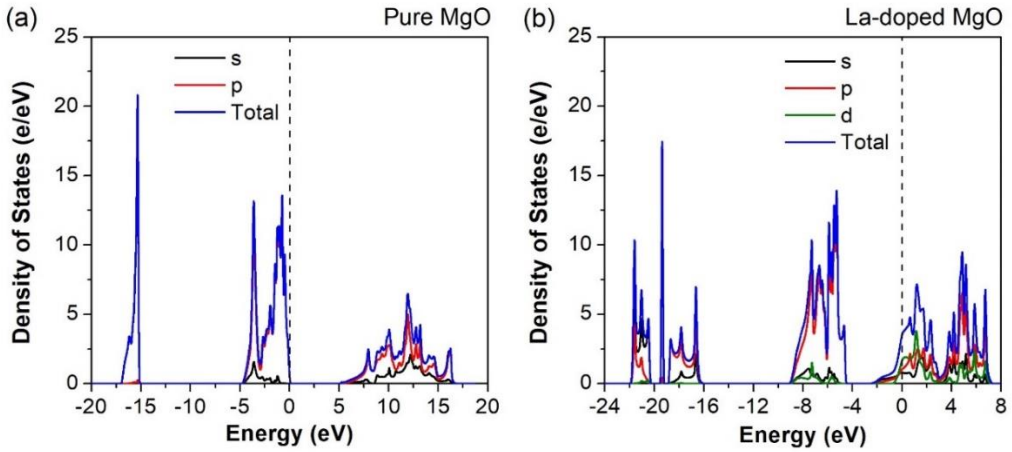

Figure 6. Total and partial DOS of (a) pure MgO and (b) La-doped MgO.

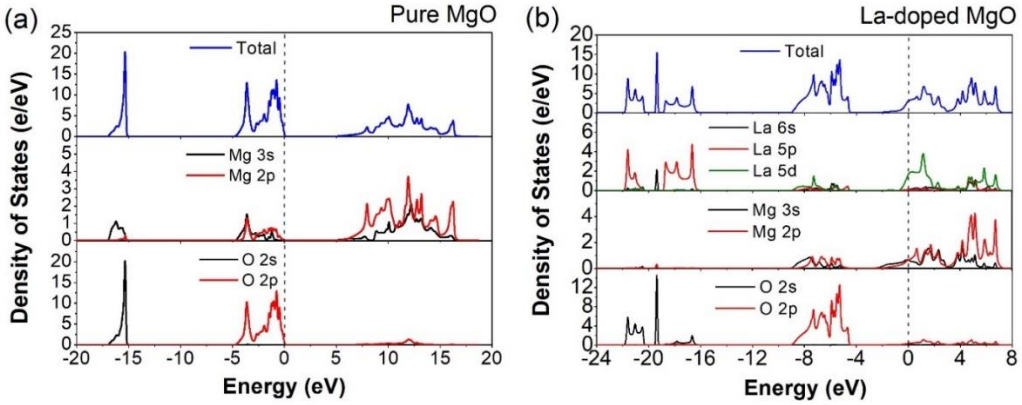

Figure 7. Total and partial DOS for La, Mg and O atoms.

3.1.3 Optical Properties

The optical properties for the absorption coefficient derived from the effect of light passing through the MgO were analyzed for the pure and La-doped MgO as shown in Figure 8 and 9 for absorption versus energy and wavelength, respectively. It is difficult to obtain the exact optical absorption due to the underestimation of the band gap. Therefore, the results of optical absorption were corrected by scissors operator [45] (scissors operator = 7.8 eV – 4.756 eV = 3.044 eV) where 7.8 is the experimental band gap (7.8 eV) [41]. The scissor operator was introduced to shift all the conduction levels to match the measured value of the band gap. The absorption coefficient α(ω) determines how far light of a particular wavelength can penetrate a material before it is absorbed. The absorption of MgO occurs in the UV light region. After La doping, the absorption edge shift towards lower energy or longer wavelength spectrum. This is consistent with the recent experimental results reports by Vaizoğullar [16] where the UV-vis spectra of La-doped MgO were red-shifted due to the presence of secondary La_2O_3 phase which can remarkably increase the photocatalytic performance of MgO. Therefore, more sunlight can be absorbed by La-doped MgO compare to pure MgO.

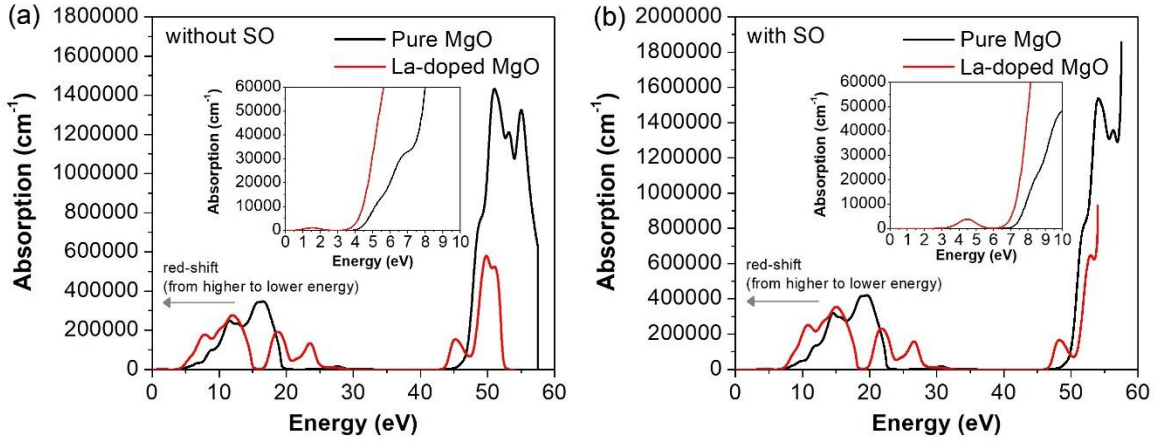

Figure 8. The optical absorption coefficient of the pure MgO and La-doped MgO against energy (eV) (a) without scissors and (b) with scissors operator.

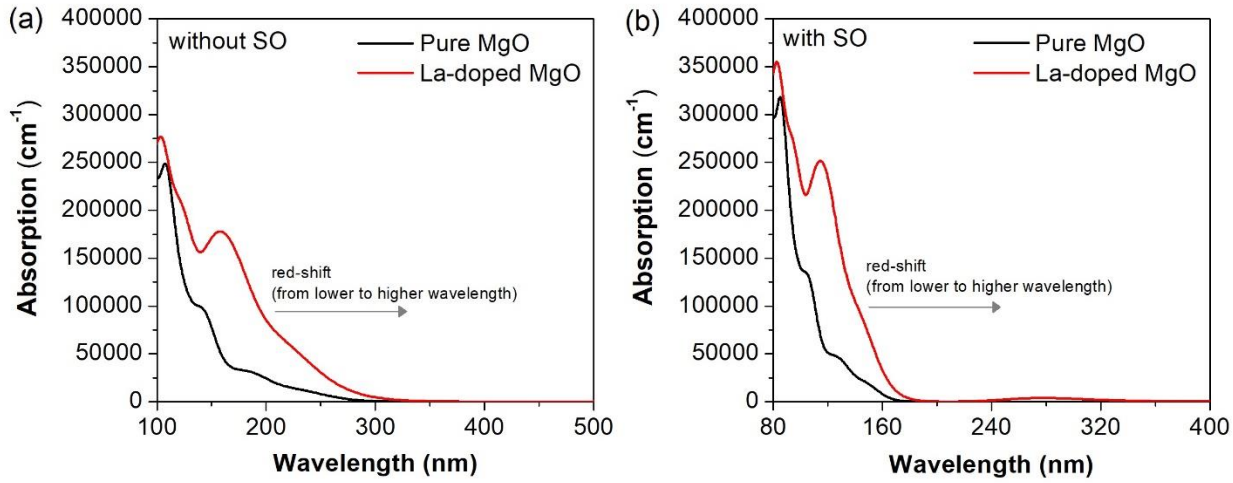

Figure 9. The optical absorption coefficient of the pure MgO and La-doped MgO against energy (eV) (a) without scissors and (b) with scissors operator.

4. CONCLUSION

In summary, the structural, electronic and optical properties of pure MgO and La-doped MgO were calculated using the first-principles study based on DFT. The calculations were performed using CASTEP by using three exchange-correlation functionals which are LDA, GGA PBE and GGA-PBEsol. The pure MgO has low optical absorption due to its wide band gap Thus, La atom was substituted into Mg to improve its optical properties. The LDA functional was used as the exchange-correlation functional to report the properties of La-doped MgO because it shows the closest value of the lattice parameter and band gap with the experimental values. The absorption edges of La-doped MgO shifted toward longer wavelength spectrum which extended from UV light. This result gives a good explanation of the red-shift of the light absorption in La-doped MgO and also may be helpful to provide atomic level understanding on the structural, electronic and optical properties of MgO and La-doped MgO for photocatalyst applications.

ACKNOWLEDGEMENTS

The authors would like to thank Universiti Teknologi MARA (UiTM) for funding and the facilities provided.

REFERENCES

[1] Wang, J., Tu, Y., Yang, L., & Tolner, H., J. Comput. Electron. **15**, 4 (2016) 1521–1530.
[2] Zheng, L., & Zhu, Y., Int. J. Electrochem. Sci. **14,** 9 (2019) 9030–9041.
[3] EL-Etre, A. Y., Reda, S. M., Ali, A. I., Helal, G. A., J. Basic Environ. Sci. **4** (2017) 311–317.
[4] Sun, D., Leng, Y., Sang, Y., Kang, X., Liu, S., Qin, X., Cui, K., Anuar, W. H., B. K., Liu, H., Bi, Y., CrystEngComm. **15**, 37 (2013) 7468–7474.
[5] Chen, X., Ng, A. M. C., Djurišić, A. B., Chan, W. K., Fong, P. W. K., Lui, H. F., Surya, C., Cheng, C. C. W., Kwok, W. M., Thin Solid Films **527** (2013) 303–307.
[6] Julkapli, N. M., Bagheri, S., Rev. Inorg. Chem. **36**, 1 (2016) 1–41.
[7] Zhang, D.-N., Zhao, L., Wang, J.-F., Li, Y.-L, Surf. Rev. Lett. **22,** 03 (2015) 1550037.
[8] Roessler, D. M., & Walker, W. C., Phys. Rev. **159**, 3 (1967) 733–738.
[9] Baysal, T., Noor, N., & Demir, A., Polym. Technol. Mater., (2020) 1–30.

[10] Mageshwari, K., Sathyamoorthy, R., Trans. Indian Inst. Met. **65**, 1 (2012) 49–55.
[11] Arani, A. A. A., Alirezaie, A., Kamyab, M. H., Motallebi, S. M., Phys. A Stat. Mech. its Appl. **554** (2020) 123950.
[12] Liu, G., Ji, S., Yin, L., Fei, G., Ye, C., J. Phys. Condens. Matter **22**, 4 (2010) 046002.
[13] Rani, N., Chahal, S., Kumar, P., Shukla, R., & Singh, S. K., J. Supercond. Nov. Magn. 33, 5 (2020) 1473–1480.
[14] P. Kaur, A. Kaur, S. Thakur, S. Singh, & L. Singh, "Structural and optical behaviour of pure and iron doped MgO nanophosphors," in 3Rd International Conference on Condensed Matter and Applied Physics (ICC-2019) 020040.
[15] Xu, K., Yang, P., Peng, W., Li, L., J. Alloys Compd. **829** (2020) 154516.
[16] Vaizoğullar, A. İ., J. Electron. Mater. 47, 11 (2018) 6751–6758.
[17] Liu, X. Q., Zhang, R. F., Su, Y. G., & Wang, X. J., Adv. Mater. Res. **233–235** (2011) 2119–2124.
[18] Deng, S. H., Duan, M. Y., Xu, M., & He, L., Phys. B Condens. Matter **406,** 11 (2011) 2314–2318.
[19] Wei P., Zeng, Y., Zhang, C.-B., Yan, Y.-H., & Hu, W., Int. J. Phys. Sci. **7**, 14 (2012) 2174–2180.
[20] Ahsaine, H. A., Slassi, A., Naciri, Y., Chennah, A., Jaramillo-Páez, C., Anfar, Z., Zbair, M., Benlhachemi, A., & Navío, J. A., ChemistrySelect **3,** 27 (2018) 7778–7791.
[21] Chen, C. P., Qi, M. L., Adv. Mater. Res. 393–395 (2011) 80–83.
[22] Huang, P., Shang, B., Li, L., & Lei, J., Chinese J. Chem. Phys. **28,** 6 (2015) 681–687.
[23] Armaković, S. J., Grujić-Brojčin, M., Šćepanović, M., Armaković, S., Golubović, A., Babić, B., Abramović, B. F., Arab. J. Chem. **12**, issue 8 (2019) 5355–5369.
[24] Liu, R. X., Wang, X. C., Chen, G. F., & Yang, B. H., Phys. E Low-Dimensional Syst. Nanostructures **74** (2015) 226–232.
[25] Hussin, N. H., Taib, M. F. M., Samat, M. H., Jon, N., Hassan, O. H., Yahya, M. Z. A., Appl. Mech. Mater. **864** (2017) 127–132.
[26] Xie, H. Q., Zeng, Y., Huang, W. Q., Peng, L., Peng, P., & Wang, T. H., Int. J. Phys. Sci. **5**, 17 (2010) 2672–2678.
[27] Ahmed, A. J., Nazrul Islam, S. M. K., Hossain, R., Kim, J., Kim, M., Billah, M., Hossain, M. S. A., Yamauchi, Y., & Wang, X., R. Soc. Open Sci. **6,** 10 (2019) 190870.
[28] Ghosh, A., Trujillo, D. P., Choi, H., Nakhmanson, S. M., Alpay, S. P., Zhu, J.-X., Sci. Rep. **9**, 1 (2019) 194.
[29] Clark, S. J., Segall, M. D., Pickard, C. J., Hasnip, P. J., Probert, M. I. J., Refson, K., Payne, M., Zeitschrift für Krist. - Cryst. Mater. **220** (2005) 567–570.
[30] Ceperley, D. M., Alder, B. J., Phys. Rev. Lett. **45**, 7 (1980) 566–569.
[31] Perdew, J P, Zunger, A., Phys. Rev. B **23**, 10 (1981) 5048–5079.
[32] Perdew, John P., Burke, K., Ernzerhof, M., Phys. Rev. Lett. 77, 18 (1996) 3865–3868.
[33] Perdew, John P., Ruzsinszky, A., Csonka, G. I., Vydrov, O. A., Scuseria, G. E., Constantin, L. A., Zhou, X., Burke, K., Phys. Rev. Lett. **100**, 13 (2008) 136406.
[34] Oganov, A. R., Gillan, M. J., & Price, G. D., J. Chem. Phys. **118**, 22 (2003) 10174–10182.
[35] Zobel, N., Behrendt, F., J. Chem. Phys. **125,** 7 (2006) 074715.
[36] Yang, B., Peng, X., Huang, C., Yin, D., Zhao, Y., Sun, S., Yue, X., Fu, T., Comput. Mater. Sci. **150**, December 2017 (2018) 390–396.
[37] Khalfallah, B., Khodja, F. D., Doumi, B., Berber, M., Mokaddem, A., Bentayeb, A., J. Comput. Electron. **17**, 3 (2018) 899–908.
[38] van Huis, M. A., van Veen, A., Schut, H., Kooi, B. J., & De Hosson, J. T. M., Phys. Rev. B **67**, 23 (2003) 235409.
[39] Chen, W., Yuan, P., Zhang, S., Sun, Q., Liang, E., Jia, Y., Phys. B Condens. Matter **407**, 6 (2012) 1038–1043.
[40] Dronskowski, R., Mater. Today **9**, 3 (2006) 53.
[41] Heo, S., Cho, E., Lee, H. I., Park, G. S., Kang, H. J., Nagatomi, T., Choi, P., & Choi, B. D., AIP Adv. **5**, 7 (2015).
[42] Århammar, C., Moyses Araujo, C., Rao, K. V., Norgren, S., Johansson, B., & Ahuja, R., Phys. Rev. B - Condens. Matter Mater. Phys. **82**, 13 (2010) 1–9, 2010.
[43] Taib, M. F. M., Mustaffa, D. T., Hussin, N. H., Samat, M. H., Ali, A. M. M., Hassan, O. H., Yahya, M. Z. A., Mater. Res. Express **6**, 9 (2019) 094012.

[44] Dadsetani, M., Beiranvand, R., Solid State Sci. **11**, 12 (2009) 2099–2105.
[45] Godby, R. W., Schlüter, M., & Sham, L. J., Phys. Rev. B **37**, 17 (1988) 10159–10175.